Publishing Excellence Inspiring Progress
ARISTON PUBLICATIONS
Energy & Environment Advances
ISSN: 3066-5728 https://aristonpubs.com/energy-environment-advances https://doi.org/10.69626/eea.2024.0049

RESEARCH ARTICLE

Comparative Analysis of Earth–Abundant Kesterite Solar Cells: Performance Evaluation of CZTS/CZTSe/CZTSSe Absorber Layers Using SCAPS–1D

Shweta Yadav *, R. K. Chauhan, Rajan Mishra

ABSTRACT: This study presents a comparative performance analysis of kesterite-based solar cells, utilizing absorber layers of CZTS, CZTSe, and CZTSSe. Kesterite materials, renowned for their earth abundance, non-toxicity, and cost-effectiveness, hold significant promise as p-type absorbers in photovoltaic applications. Their direct bandgap, adjustable between 1.0 eV and 1.5 eV by tailoring the selenium-to-sulfur ratio, makes them suitable for high-efficiency solar cells. The simulated device structure comprises ZnO:Al as the window layer, ZnSe as the buffer layer, CZTS/CZTSe/CZTSSe as the absorber layers, and graphene oxide (GO) as the hole transport layer (HTL). Through SCAPS-1D simulations, key parameters such as open-circuit voltage (Voc), short-circuit current density (Jsc), fill factor (FF), and power conversion efficiency (PCE) are analyzed. The study further investigates the effects of absorber thickness, doping concentration of the absorber, electron transport layer (ETL), and HTL, as well as series and shunt resistances. Among the studied configurations, the CZTSSe-based solar cell demonstrates superior performance with a Voc of 0.9367 V, Jsc of 37.44 mA/cm², FF of 82.68%, and a PCE of 30.01%. This research highlights the pivotal role of material composition and device optimization in achieving high-efficiency solar cells. The findings provide valuable insights for the development of advanced kesterite-based photovoltaics, identifying CZTSSe as the most promising absorber material for next-generation solar cells due to its superior performance metrics and tunable properties.

Keywords: Thin-film Solar Cell, CZTS, CZTSe, CZTSSe, SCAPS-1d, Conversion efficiency.

Received: 25 February 2024; Revised: 17 March 2024; Accepted: 12 April 2024; Published Online: 03 May 2024

1. INTRODUCTION

In recent years, there has been a remarkable surge in interest within the research community concerning photovoltaic (PV) thin films [1]. This attention stems from their numerous advantageous properties, including cost-effective production, relatively simple fabrication processes, and efficiency levels that rival other established solar cell technologies [2]. The growing need for sustainable and renewable energy sources to combat climate change has further fueled interest in advancing thin-film PV technologies. Among the various materials explored for solar cells, kesterite compounds have emerged as a promising candidate due to their unique combination of material abundance, environmental compatibility, and excellent optoelectronic properties [3, 4].

Kesterite materials, particularly $Cu_2ZnSn(SxSe_{1-x})_4$, have gained significant attention in the field of photovoltaics. These quaternary semiconductors, which include Cu_2ZnSnS_4 (CZTS), $Cu_2ZnSnSe_4$ (CZTSe), and their alloy $Cu_2ZnSn(SxSe_{1-x})_4$ (CZTSSe), exhibit extraordinary potential as absorber layers in thin-film solar cells [5-7]. The tunable bandgap of kesterite materials, which can be adjusted within the range of 1.0–1.5 eV by modifying the sulfur-to-selenium ratio, makes them particularly suitable for photovoltaic applications. This range aligns closely with the optimal bandgap for solar energy conversion, thereby

Department of Electronics & Communication Engineering, Madan Mohan Malaviya University of Technology, Gorakhpur-273010, Uttar Pradesh, India.

* Author to whom correspondence should be addressed: Shwetay0842@gmail.com (Shweta Yadav)

© Ariston Publications 2024. All rights reserved.

enabling effective absorption of sunlight and improved power conversion efficiency [8].

Another critical advantage of kesterite-based materials is their earth abundance and environmental compatibility. Unlike conventional thin-film absorbers such as CdTe and CIGS (copper indium gallium diselenide), kesterites do not rely on scarce or toxic elements [9]. Instead, they are composed of readily available elements—copper, zinc, tin, sulfur, and selenium—which are abundant in Earth's crust. This abundance not only ensures the sustainability of kesterite-based solar cells but also positions them as cost-effective alternatives to other thin-film technologies. Additionally, the absence of toxic components, such as cadmium, makes kesterite solar cells more environmentally friendly, aligning with global efforts to reduce hazardous waste and promote green energy solutions [10].

The optical and electronic properties of kesterite materials further enhance their attractiveness for photovoltaic applications. These materials exhibit strong light absorption coefficients ($>10^4$ cm^{-1}), allowing them to absorb a significant portion of the solar spectrum within a thin absorber layer. Moreover, their direct bandgap facilitates efficient charge carrier generation, while their tunable composition enables optimization for various operational conditions. The combination of these properties positions kesterite compounds as one of the most promising materials for next-generation thin-film solar cells [11, 12].

Despite these advantages, challenges remain in optimizing the performance of kesterite-based solar cells. Issues such as high defect density, suboptimal band alignment, and non-uniform elemental distribution can limit device performance [13, 14]. Additionally, the presence of secondary phases and intrinsic defects, such as Cu/Zn disorder and deep-level traps, can adversely affect the open-circuit voltage (Voc) and fill factor (FF), thereby reducing the overall power conversion efficiency (PCE). As a result, extensive research has been conducted to overcome these limitations through material engineering, process optimization, and device simulation [15-17].

In this context, CZTS, CZTSe, and CZTSSe absorber layers have been extensively studied, with many research papers demonstrating their potential for high-performance solar cells [18]. The alloy CZTSSe, in particular, has garnered significant attention due to its ability to combine the favorable properties of both CZTS and CZTSe. By adjusting the sulfur-to-selenium ratio, CZTSSe can achieve an optimal balance between bandgap energy, light absorption, and carrier mobility, making it a versatile material for PV applications.

To further enhance the performance of kesterite-based solar cells, researchers have explored innovative device architectures and alternative buffer layers. One notable advancement is the replacement of the toxic cadmium sulfide (CdS) buffer layer with more environmentally friendly materials such as zinc selenide (ZnSe). ZnSe not only eliminates the environmental concerns associated with CdS but also offers superior band alignment with kesterite absorbers, resulting in improved charge carrier collection and reduced interface recombination [19-21].

In this study, we present a detailed comparative analysis of kesterite-based solar cells employing CZTS, CZTSe, and CZTSSe as absorber layers. The simulated device structure consists of ZnO:Al/ZnSe/(CZTS/CZTSe/CZTSSe)/graphene oxide (GO), where ZnSe serves as the buffer layer, ZnO:Al acts as the transparent conducting oxide (TCO), and GO functions as the hole transport layer (HTL). Using the SCAPS-1D simulator, we systematically investigate the impact of various device parameters, including absorber layer thickness, doping concentration, and series and shunt resistances, on the overall device performance. Key performance metrics, including open-circuit voltage (Voc), short-circuit current density (Jsc), fill factor (FF), and power conversion efficiency (PCE), are computed for each configuration. The study also examines the influence of material composition on defect density, band alignment, and carrier transport properties. The results are compared with previously reported values, providing a comprehensive understanding of the advantages and limitations of each absorber layer.

Our findings reveal that the CZTSSe-based solar cell demonstrates superior performance compared to its CZTS and CZTSe counterparts. Specifically, the CZTSSe absorber layer achieves a Voc of 0.9367 V, a Jsc of 37.44 mA/cm², an FF of 82.68%, and a PCE of 30.01%. These results highlight the potential of CZTSSe as the most promising absorber material for high-efficiency kesterite solar cells. By providing a detailed analysis of kesterite-based solar cells and identifying the critical factors influencing their performance, this study contributes to the advancement of sustainable and cost-effective photovoltaic technologies. The insights gained from this work offer valuable guidance for the design and optimization of next-generation thin-film solar cells, paving the way for their widespread adoption in renewable energy systems.

2. DEVICE LAYOUT AND MATERIAL PROPERTIES

The SCAPS-1D software, a tool developed by University of Ghent, numerically solves the Poisson, continuity, and carrier transport equations to characterize solar cell devices [11, 23]. This study introduces and simulates various solar cell structures (Front contact/ZnO: Al/ZnSe/ (CZTS/CZTSe/ CZTSSe)/GO/back contact) utilizing alternative absorber materials, illustrated in Figure 1 (a). Additionally, enhanced material characteristics used in this simulation is listed in Table 1. Simulation of these devices is conducted under standard conditions, with an illumination spectrum power equivalent to one sun (1000 W/m^2) and utilizing Air Mass 1.5 global spectrum. The operating temperature set at 300 K, and devices are positioned precisely perpendicular to incident sunlight [16]. The corresponding band alignment and energy band gap are presented in Figures 1 (b) and (c), respectively.

 © Ariston Publications 2024. All rights reserved

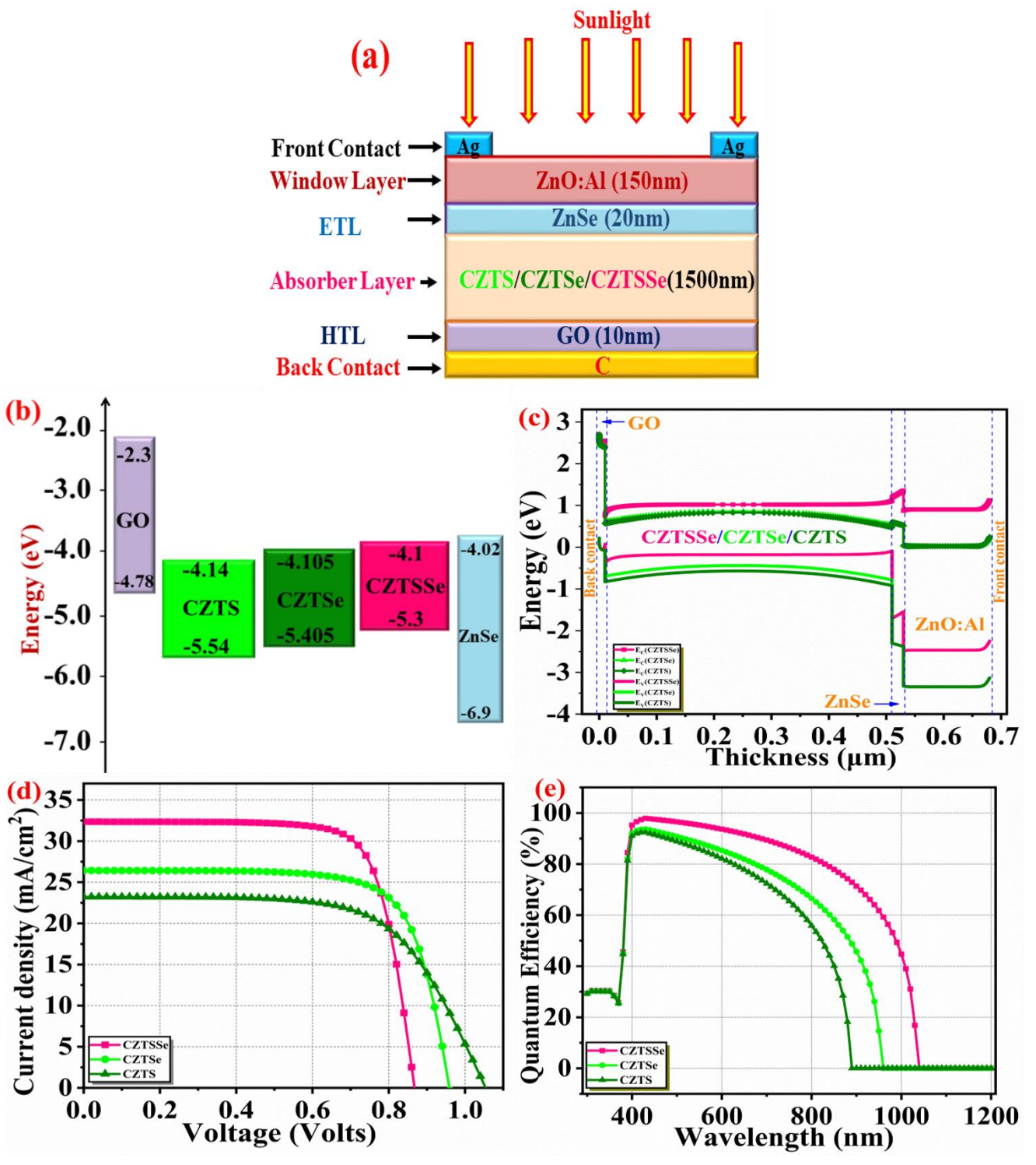


Fig. 1. (a) Device geometry, (b) band energy diagram, (c) bandgap, (d) current-voltage response, and (e) external quantum efficiency of the CZTSSe solar cell.

Band alignment in solar cell refers to arrangement of energy levels of semiconductor materials at their interfaces. It determines how effectively electrons and holes can move between layers, crucial for generating electrical current when exposed to sunlight. Achieving optimal band alignment is essential for maximizing solar cell efficiency, accomplished through careful selection and engineering of semiconductor materials and interface control. The energy band gap of a solar cell is minimum energy difference between valence band and conduction band of its semiconductor material. It determines energy of photons that can be absorbed to generate electron-hole pairs, crucial for solar cell operation. In Figures 1(d) and (e), J-V and QE with different absorber layers are depicted.

© Ariston Publications 2024. All rights reserved.

Table 1. The parameters utilized in this investigation.

Parameters	**GO**	**CZTSSe**	**CZTSe**	**CZTS**	**ZnSe**	**ZnO:Al**
Thickness (nm)	10	1500			20	150
Bandgap (eV)	2.48	1.2	1.3	1.4	2.9	3.37
Electron mobility ($cm^2\ V^{-1}\ s^{-1}$)	26	100				
Dielectric permittivity (relative)	10	13.6			10	8.49
Electron thermal velocity ($cm\ s^{-1}$)	5.2×10^7	1×10^7				
Electron affinity (eV)	2.3	4.1	4.105	4.14	4.02	4.5
Conduction band effective density of states (cm^{-3})	2.2×10^{18}					
Hole mobility ($cm^2\ V^{-1}\ s^{-1}$)	123	25				
Shallow uniform acceptor density, N_A (cm^{-3})	1×10^{17}	1×10^{18}			0	
Hole thermal velocity ($cm\ s^{-1}$)	5.2×10^7	1×10^7				
Valance band effective density of states (cm^{-3})	1.8×10^{19}					
Shallow uniform donor density, N_D (cm^{-3})	0				1×10^{17}	1×10^{18}
Defect density (cm^{-3})	1×10^{14} (n)					1×10^{17}(A)
Key matrices of the suggested solar device					S_n (cm/s)	S_p (cm/s)
Front Contact					10^7	10^5
Back Contact					10^5	10^7

3. RESULTS AND DISCUSSION

3.1. The Effect of Thickness on Three Different Absorbers Layers (CZTS/CZTSe/CZTSSe)

The absorber layer is essential for enhancing the efficiency the efficiency of solar devices. To investigate this, simulations were conducted using CZTS/CZTSe/CZTSSe absorber layers. Figures 2(a)–(d) demonstrates how thickness of various absorber materials varies between 0.3 and 1.8 µm. As thickness of absorber material decreases, rate of recombination increases due to a rise in dark saturation current, leading to a slight decrease in *Voc*. However, both efficiency and *Jsc* increase until reaching 1.5 µm, after which they stabilize. A thinner absorber allows electrons and holes to combine more quickly, increasing recombination rates. Conversely, thicker absorbers provide more space for photon absorption, boosting Jsc. The fill factor (FF) decreases with increasing thickness.

The relationships between key parameters like V_{OC}, J_{SC}, FF, and PCE are understood through equations 1 to 3 [5].

$$V_{oc} = \frac{KT}{q}\left[ln\left(\frac{J_{sc}}{J_o}+1\right)\right] \quad (1)$$

$$FF = \frac{P_{max}}{J_{sc}\times V_{oc}} \quad (2)$$

$$\eta = \frac{V_{oc} \times J_{sc} \times FF}{P_{in}} \quad (3)$$

Where, $\frac{KT}{q}$ is thermal voltage, J_O specifies level of reverse saturation current. P_{max} maximum power, and incoming power, that P_{in}. Optimal efficiency, reaching 23.33%, is achieved with an absorber thickness of 1.5 µm. In comparison, CZTSSe absorber layer demonstrates good efficiency with increasing thickness.

3.2. The Effect of Absorber Doping Concentration on Three Different Absorbers Layers (CZTS/CZTSe/CZTSSe)

In this segment, we observe pivotal influence of absorber layer doping on enhancing efficacy of solar devices. To delve into this matter, we carried out simulations employing CZTS/CZTSe/CZTSSe absorber layers. Figures 3 (a)–(d) depicts fluctuations in doping levels ranging from $10^{14}cm^{-3}$ to $10^{19}cm^{-3}$ across different absorber materials.

 © Ariston Publications 2024. All rights reserved

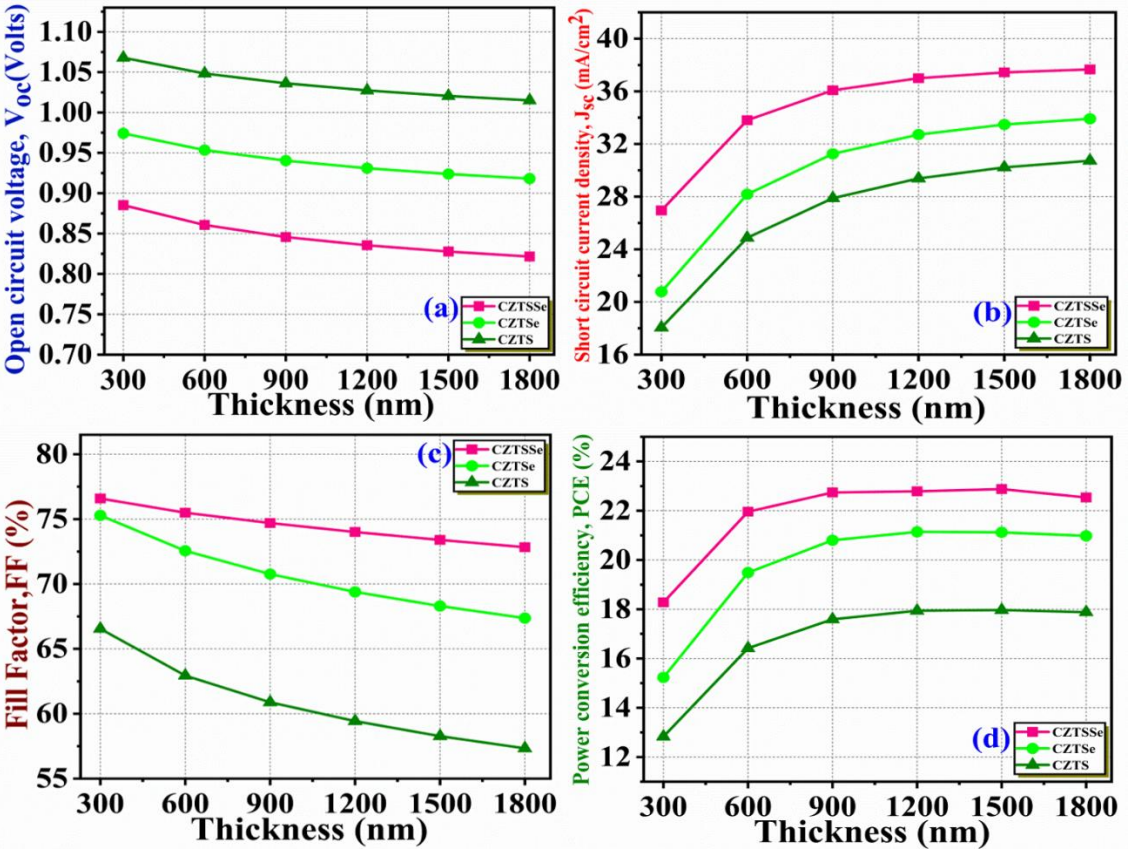


Fig. 2. Impacts of different absorber layer thickness (a) V_{OC}, (b) J_{SC}, (c) FF and (d) PCE.

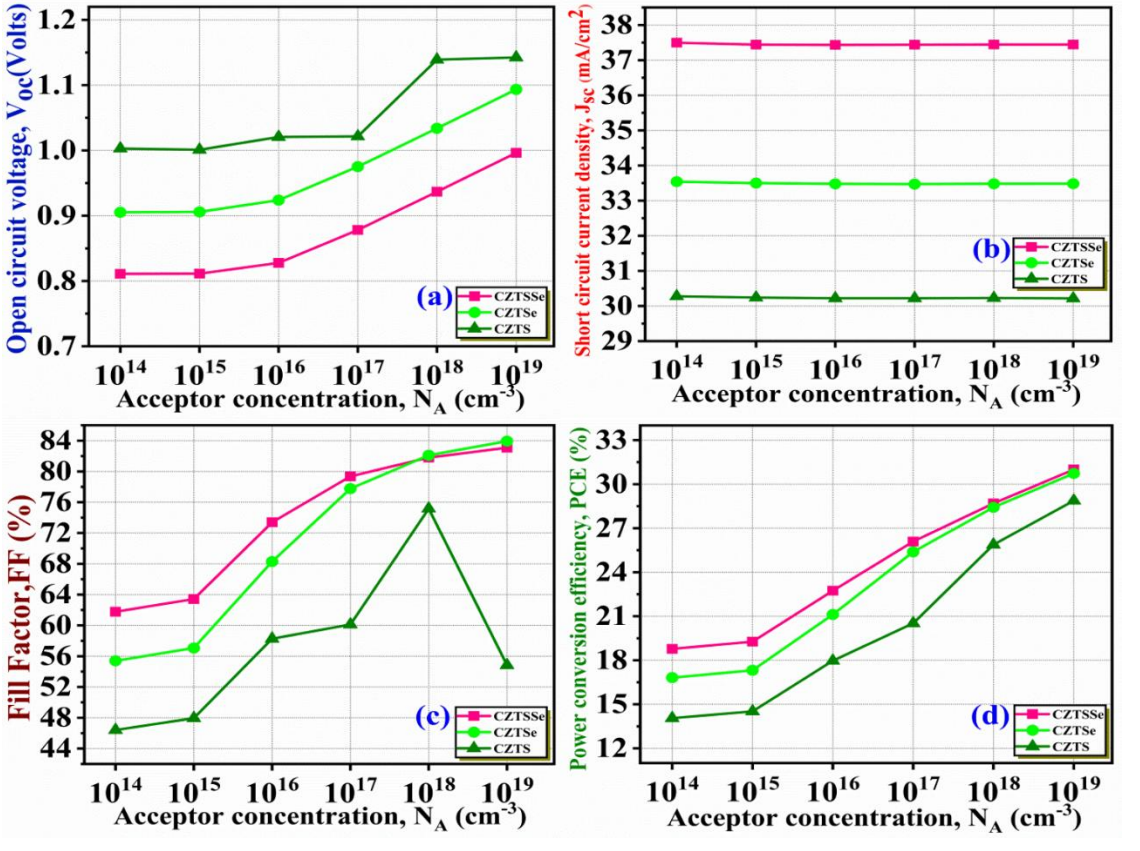


Fig. 3. Impacts of different absorber layer doping concentration on (a) V_{OC}, (b) J_{SC}, (c) FF and (d) PCE.

© Ariston Publications 2024. All rights reserved.

With increasing doping levels, Voc shows an increase in CZTSSe and CZTSe, but in CZTS, it decreases and then increases, as shown in Figure 3(a). *Jsc* exhibits minor changes across all absorber layers, as illustrated in Figure 3b. FF increases in CZTSSe and CZTSe absorber layers with increasing doping levels, whereas for CZTS, it shows both an increase and decrease with doping levels, as shown in Figure 3(c). PCE increases with increasing doping levels for CZTSSe/CZTSe/CZTS absorber layers, as depicted in Figure 3(d).

Excessive free carrier absorption, which escalates proportionally with carrier count, is likely responsible for decline in short-circuit current at elevated doping levels. Amplified doping concentration within absorber layer intensifies band-to-band recombination of photogenerated carriers. Consequently, CZTSSe absorber layers exhibit subpar solar cell properties under high doping concentrations. This investigation demonstrates that V_{OC} of solar cells experiences enhancement as doping concentration of CZTSSe absorbers increases. However, it's essential to recognize potential reduction in J_{SC} and PCE due to heightened recombination of photogenerated carriers induced by imperfections [15, 17]. In this study, absorber doping concentration of absorber layer was kept at 10^{18} cm^{-3}, considering structure size for further optimization. CZTSSe demonstrates higher conversion efficiency (28.69%) compared to other CZTSe and CZTS absorber layers.

3.3. The Effect of ETL Doping Concentration on Three Different Absorbers Layers (CZTS/CZTSe/CZTSSe)

The role of buffer layer in thin-film solar cells is crucial as it facilitates generation of p-n junction, which is responsible for electrons and holes within the device. ZnSe, with its higher bandgap compared to absorber layer, enables more light to reach junction area, enhancing generation of electron-hole pairs through photon absorption. While a thin buffer layer is preferred to maintain minimal thickness [20], too thin layers can lead to leakage current issues. Hence, to strike a balance, thickness of buffer layer remains constant at 20nm for CZTS/CZTSe/CZTSSe absorber layers.

In this section, we investigate how doping concentration of buffer layer affects solar cell parameters across three distinct absorber layers. Figures 4 (a)-(d) showcases alteration in solar cell performance as doping concentration (cm^{-3}) of buffer layer increases. Additionally, Figures 4 (a)-(d) present variations in electrical characteristics (FF, J_{SC}, V_{OC}, and efficiency) as electron concentration ranges from 10^{14} to 10^{19} cm^{-3} for CZTS/CZTSe/CZTSSe absorber layer structures. The augmentation of doping level in CZTSSe absorber layer amplifies built-in electric field within solar cell devices, potentially enhancing Voc. While maintaining a constant defect density, an increase in absorber layer absorption results in a linear decline in V_{OC}. Similarly, J_{SC} is anticipated to exhibit a linear trend.

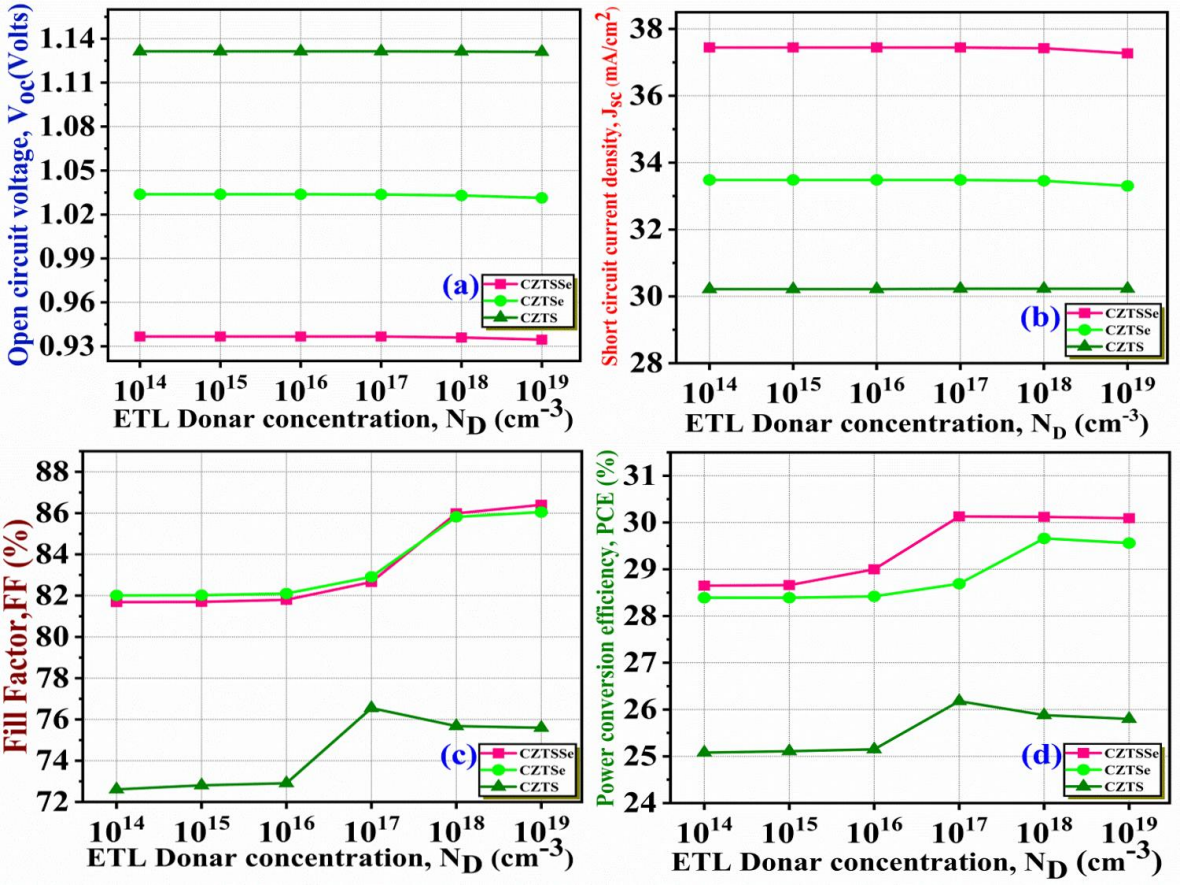


Fig. 4. Impacts of different absorber layer on ETL doping concentration on (a) V_{OC}, (b) J_{SC}, (c) FF and (d) PCE.

 © Ariston Publications 2024. All rights reserved

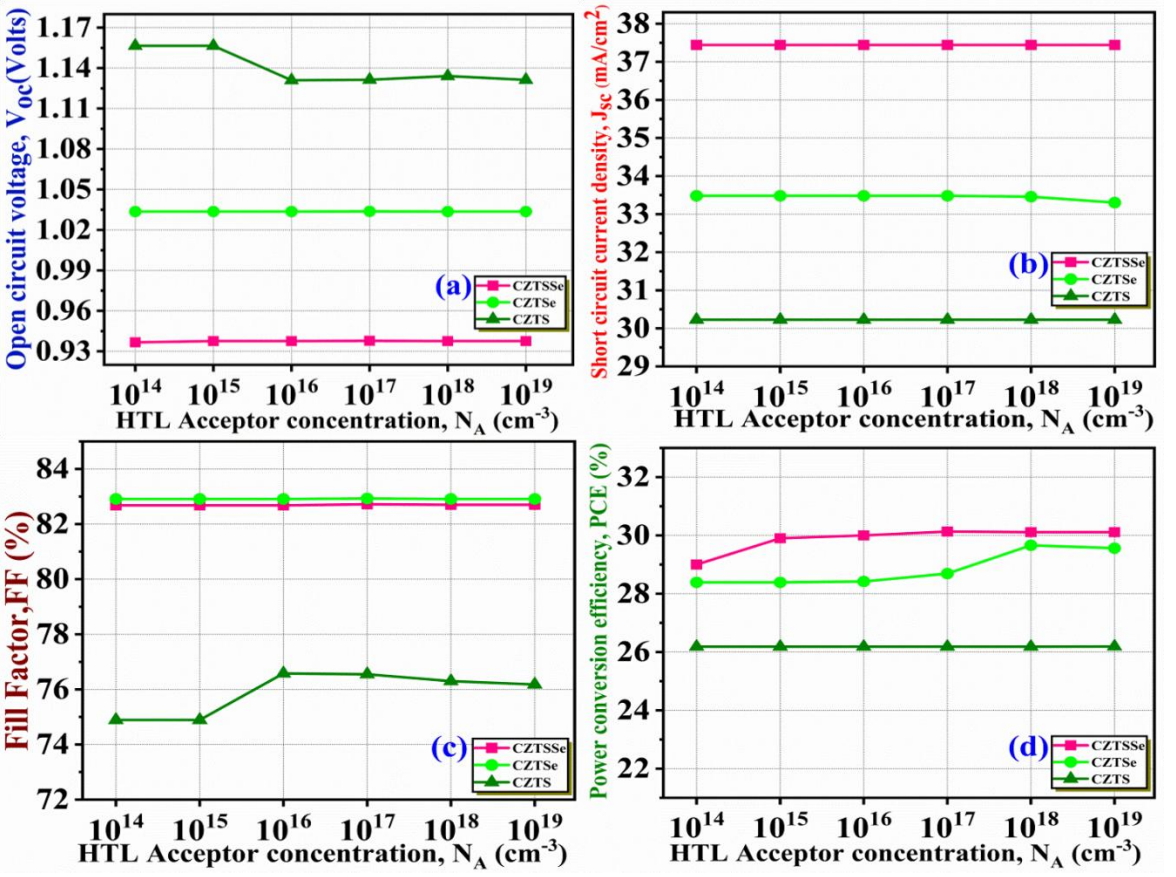


Fig. 5. Impacts of different absorber layer on ETL doping concentration on (a) Voc, (b) Jsc, (c) FF and (d) PCE.

However, as defect density rises, Shockley-Read-Hall recombination also enhance, leading to heightened band-to-band recombination with higher doping concentrations in absorber layer [9]. Figures 4 (a)-(d) highlight that CZTSSe exhibits superior conversion efficiency (30.01%) compared to other absorber layers (CZTSe, CZTS) and establishes a doping concentration of 10^{17} cm^{-3} for subsequent optimization.

3.4. The Effect of HTL Doping Concentration on Three Different Absorbers Layers (CZTS/CZTSe/CZTSSe)

Our proposal suggests employing a graphene oxide (GO) film a hole transport layer in solar cells with three different absorber layers (CZTS/CZTSe/CZTSSe) and evaluating its effect on their performance. GO emerges an appropriate material to tackle unfavorable interfacial challenges typically observed in CZTSSe PV cells. A suitably thick GO film maintains transparency and without compromises sheet resistivity of back contact. Furthermore, GO exhibits compatibility with absorber layers, enabling it to function effectively as a hole transfer layer. For this study HTL thickness kept constant at 10nm for three different absorber layers. Figures 5a-d shows doping concentration between 10^{14} to 10^{19} cm^{-3} electrical parameters effect on CZTS/CZTSe/CZTSSe absorber layer.

Figures 5 (a) and (b) illustrate that as acceptor carrier level in HTL layer enhanced, J_{SC} remains nearly constant. Similarly, V_{OC} show constant correlations regarding HTL doping concentration. These observations suggest that variations in acceptor doping density have minimal impact on J_{SC} and V_{OC}, implying that recombination rate among PV device is independent of acceptor concentration and mainly affected by conduct of minority carriers. Additionally, Figures 5 (c) and (d) show minor enhancement in FF and efficiency with increasing doping level. This indicates a slight improvement in FF and efficiency at higher carrier concentrations. This behavior can be attributed to decline in recombination at PV device back surface, arising from elevated acceptor doping density [14]. Our exhaustive analysis has identified that preferable acceptor concentration for HTL layer is 10^{17} cm^{-3}. Furthermore, CZTSSe absorber layer exhibits superior performance (PCE 30.01%) compared to other absorber layers (CZTSe, CZTS).

3.5. The Effect of Rs and Rsh on CZTSSe Absorbers Layer

After reviewing performance of all above subsections, it is obvious that CZTSSe absorber layer exhibits superior performance when compared to CZTSe and CZTS. This section examines solar cell's series and shunt resistance.

© Ariston Publications 2024. All rights reserved.

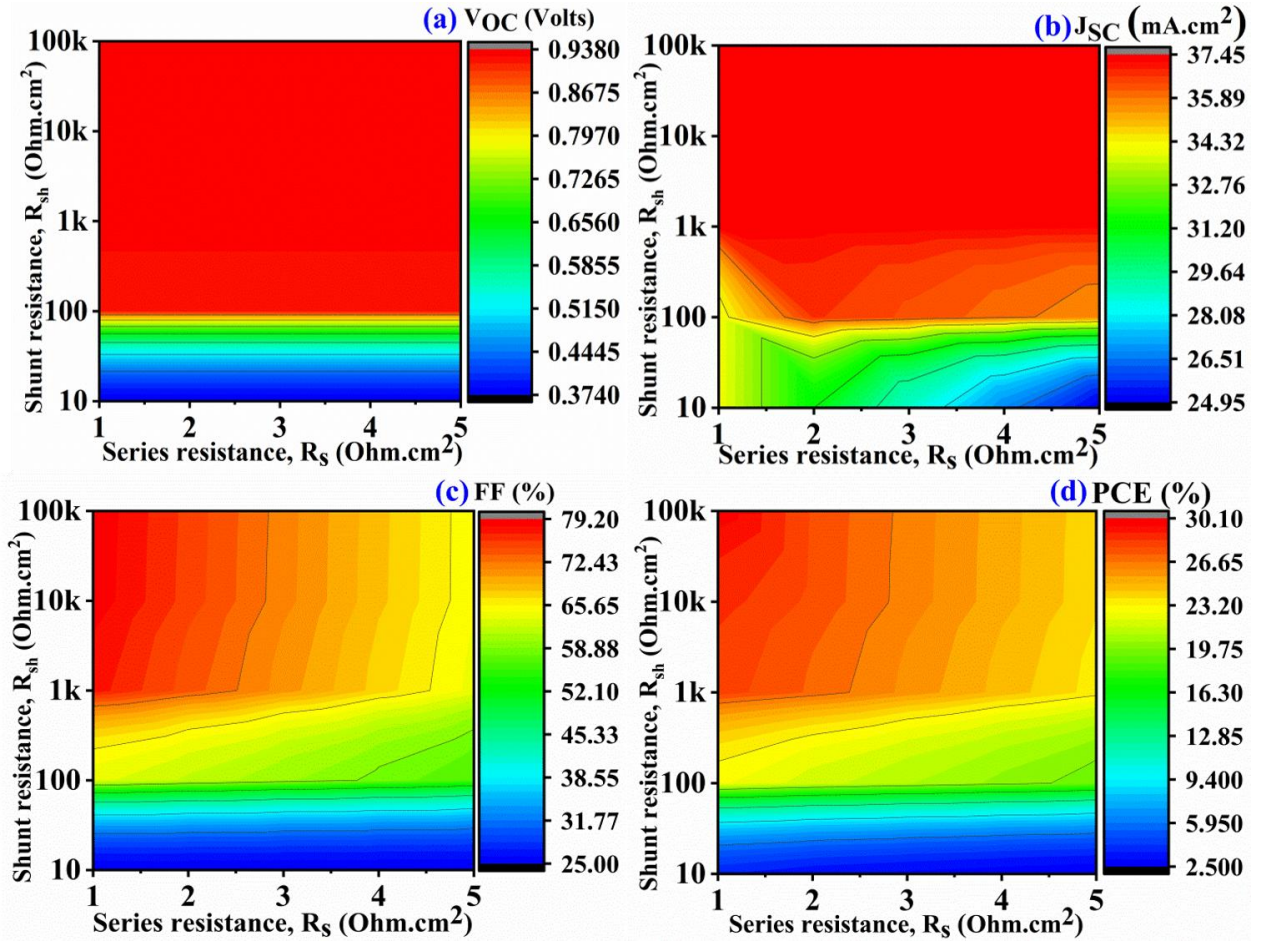


Fig. 6. Impacts of CZTSSe absorber layer on Rs and Rsh on (a) Voc, (b) Jsc, (c) FF and (d) PCE.

The simulation varied shunt resistance between 1 and 5 (cm^2) and series resistance between 10 and 10^5 (cm^2). Figures 6 (a)–(d) show changes in solar cell specifications resulting from these variations. Series resistance (Rs) is affected by factors like bulk resistance and electrode configuration, while shunt resistance (Rsh) relates to recombination at defect levels [6]. Increasing Rsh correlates with reduced defect levels. In Figure 6 (a), increasing series resistance initially reduces V_{OC}, and then stabilizes. Up to 10^2 cm^2, higher Rsh increases V_{OC}, with minimal effect beyond. Figure 6b shows J_{SC} decreasing as both Rs and Rsh increase up to 10^2 Ω cm^2.Figures 6c,d shows FF and efficiency decrease with rising Rs, but increase with Rsh up to 10^3 Ω cm^2, with marginal gains thereafter. High Rs reduces J_{SC}, while low Rs decrease V_{OC}, leading to lower FF and poor performance. Minimizing Rs and maximizing Rsh enhances solar cell efficiency and minimizes losses. The current output of the CZTSSe photovoltaic cell, which includes a ZnSe electron transport layer (ETL) and a graphene oxide (GO) hole transport layer (HTL), can be elucidated using equation (4) [7, 13]:

$$I = I_{ph} - \frac{V + IR_s}{R_{sh}} - I_O\left[e^{\left(\frac{V + IR_s}{nV_{th}}\right)} - 1\right] \quad (4)$$

Here, I_{ph} represents photogenerated current, V symbolizes voltage across the cell, *Rs* and *Rsh* respectively denote series and shunt resistances. The reverse saturation current is represented by I_O, diode quality factor is denoted by n, and thermal voltage is represented by V_t.

4. CONCLUSION

This paper presents a comprehensive analysis of kesterite-based solar cells, focusing on CZTS, CZTSe, and CZTSSe absorber layers. Kesterites, as earth-abundant, non-toxic, and cost-effective materials, offer significant potential for photovoltaic applications. Their adjustable direct bandgap, ranging from 1.0 eV to 1.5 eV by modulating the selenium-to-sulfur ratio, makes them suitable candidates for high-efficiency solar cells. Using SCAPS-1D simulations, we evaluated the performance of solar cells with a ZnO:Al/ZnSe/(CZTS/CZTSe/CZTSSe)/GO structure. Key performance metrics, including open-circuit voltage (Voc), short-circuit current density (Jsc), fill factor (FF), and power conversion efficiency (PCE), were analyzed under various absorber layer compositions. The study also assessed the impact of critical parameters, such as absorber layer thickness (optimized at 1500 nm), doping concentrations for

 © Ariston Publications 2024. All rights reserved

the absorber (1E18), ETL (1E17), and HTL (1E17), along with series and shunt resistances. The findings reveal that the CZTSSe absorber layer outperforms CZTS and CZTSe, achieving a Voc of 0.9367 V, Jsc of 37.44 mA/cm², FF of 82.68%, and a PCE of 30.01%. The superior performance of CZTSSe is attributed to its optimal bandgap, enhanced charge carrier dynamics, and reduced recombination losses. This study underscores the importance of material selection and device optimization in advancing kesterite-based solar cells. The results not only identify CZTSSe as the most promising absorber material but also provide a roadmap for optimizing device parameters to achieve high-performance photovoltaic devices. These insights hold significant implications for the future development of cost-effective and sustainable solar energy technologies.

DECLARATIONS

Ethical Approval

We affirm that this manuscript is original work, has not been published previously, and is not currently being considered for publication in any other journal or conference proceedings. All authors have reviewed and approved manuscript, and author order has been mutually agreed upon.

Funding

Not applicable

Availability of data and material

All of the data obtained or analyzed during this study is included in the report that was submitted.

Conflicts of Interest

The authors declare that they have no financial or personal interests that could have influenced the research and findings presented in this paper. The authors alone are responsible for the content and writing of this article.

Authors' contributions

All authors contributed equally in the preparation of this manuscript.

ACKNOWLEDGEMENTS

The authors acknowledge the invaluable contribution of Dr. Marc Burgelman for developing the open-source SCAPS-1D simulation tool, a powerful tool for analyzing solar cell device physics.

REFERENCES

[1] Srivastava, A., Dua, P., Lenka, T.R. and Tripathy, S.K., **2021.** Numerical simulations on CZTS/CZTSe based solar cell with ZnSe as an alternative buffer layer using SCAPS-1D. *Materials Today: Proceedings*, *43*, pp.3735-3739.

[2] Najim, A.H. and Saleh, A.N., **2019.** Study effect of window and BSF layers on the properties of the CZTS/CZTSe solar cell by SCAPS–1D. *Tikrit Journal of Pure Science*, *24*(3), pp.77-83.

[3] Abderrezek, M. and Djeghlal, M.E., **2021.** Numerical study of CZTS/CZTSSe tandem thin film solar cell using SCAPS-1D. *Optik*, *242*, p.167320.

[4] Dixit, H., Bansal, N.K., Porwal, S., Kumar, D. and Singh, T., **2023.** Performance assessment of earth-abundant Kesterite and lead-free chalcogenide-based perovskite solar cells using SCAPS-1D. *Optik*, *295*, p.171474.

[5] Et-taya, L., Benami, A. and Ouslimane, T., **2022.** Study of CZTSSe-based solar cells with different ETMs by SCAPS. *Sustainability*, *14*(3), p.1916.

[6] Gayen, R.N. and Chakrabarti, T., **2019.** Effect of series and shunt resistance on the photovoltaic properties of solution-processed zinc oxide nanowire based CZTS solar cell in superstrate configuration. *Materials Science in Semiconductor Processing*, *100*, pp.1-7.

[7] Ghani, F., Duke, M. and Carson, J., **2013.** Numerical calculation of series and shunt resistances and diode quality factor of a photovoltaic cell using the Lambert W-function. *Solar Energy*, *91*, pp.422-431.

[8] Huang, T.J., Yin, X., Qi, G. and Gong, H., **2014.** CZTS-based materials and interfaces and their effects on the performance of thin film solar cells. *physica status solidi (RRL)–Rapid Research Letters*, *8*(09), pp.735-762.

[9] Li, J., Wang, D., Li, X., Zeng, Y. and Zhang, Y., **2018.** Cation substitution in earth-abundant kesterite photovoltaic materials. *Advanced Science*, *5*(4), p.1700744.

[10] Abdullah, A.S., Ahmad, F., Ibrahim, M.H.I. and Ibrahim, M.H., **2024.** A numerical simulation of novel solid-state dye-sensitized solar cell based on kesterite as the electrolyte. *Results in Optics*, *14*, p.100625.

[11] Rana, M.S., Islam, M.M. and Julkarnain, M., **2021.** Enhancement in efficiency of CZTS solar cell by using CZTSe BSF layer. *Solar Energy*, *226*, pp.272-287.

[12] Jeong, W.L., Park, S.H., Jho, Y.D., Joo, S.K. and Lee, D.S., **2022.** The role of the graphene oxide (GO) and reduced graphene oxide (RGO) intermediate layer in CZTSSe thin-film solar cells. *Materials*, *15*(10), p.3419.

© Ariston Publications 2024. All rights reserved.

[13] Yadav, S., Chauhan, R.K. and Mishra, R., **2024.** Performance assessment of earth-abundant kesterite-based CZTSSe solar cell using graphene oxide as HTL and zinc oxysulfide as ETL. *Engineering Research Express*, *6*(3), p.035344.

[14] Riyad, M.N.H., Sunny, A., Khatun, M.M., Rahman, S. and Ahmed, S.R.A., **2023.** Performance evaluation of WS_2 as buffer and Sb_2S_3 as hole transport layer in CZTS solar cell by numerical simulation. *Engineering Reports*, *5*(5), p.e12600.

[15] Dwivedi, D.K., **2020.** Modeling of CZTSSe solar photovoltaic cell for window layer optimization. *Optik*, *222*, p.165407.

[16] Sravani, L., Routray, S., Courel, M. and Pradhan, K.P., **2021.** Loss mechanisms in CZTS and CZTSe Kesterite thin-film solar cells: Understanding the complexity of defect density. *Solar Energy*, *227*, pp.56-66.

[17] Wahid, M.F., Ahmed, N., Rahman, M.S., Al Mamun, A., Howlader, M.N. and Tareq, M.M.R., **2023.** Performance Enhancement of CZTS Solar Cell with $CuSbS_2$ Back Surface Field: A Numerical Simulation Approach. *Engineering*, *15*(9), pp.497-513.

[18] Yadav, S., Chauhan, R.K., Mishra, R. and Kumar, S., **2023.** Investigating Ag_2S quantum dot buffer layer in CZTSSe photovoltaics for enhanced performance. *Physica Scripta*, *98*(12), p.125106.

[19] Yadav, S., Chauhan, R.K., Mishra, R. and Kumar, S., **2024.** Non-toxic materials for high efficiency thin-film solar cells: CZTSSe with In_2S_3 buffer layer. *Indian Journal of Physics*, pp.1-14.

[20] Yadav, S., Chauhan, R.K. and Mishra, R., **2024.** Performance assessment of earth-abundant kesterite-based CZTSSe solar cell using graphene oxide as HTL and zinc oxysulfide as ETL. *Engineering Research Express*, *6*(3), p.035344.

[21] Yadav, S., Chauhan, R.K. and Mishra, R., **2024.** Upgrading CZTSSe solar cell performance through numerical investigation of Cu-based hole transport layers. *Micro and Nanostructures*, *195*, p.207960.

 © Ariston Publications 2024. All rights reserved